

Supplementary Materials

of

Theoretical Insights into Pt-Rh Alloy Nanoparticles: Stability, Elemental Distribution, and Catalytic Mechanisms for NO+CO Reactions

Yuzheng Li¹, Xianbao Duan^{1,*}, Liu Zhang², Caoran Li¹, Fangwen Ye¹, Zhihong Zhang², Liuqing Chen¹, Chun Du², Qingbo Wang³, Bin Shan^{2,*}

¹ Hubei Key Laboratory of Plasma Chemistry and Advanced Materials and School of Materials Science and Engineering, Wuhan Institute of Technology, Wuhan 430205, Hubei, China

² State Key Laboratory of Intelligent Manufacturing Equipment and Technology and School of Materials Science and Engineering, Huazhong University of Science and Technology, Wuhan 430074, Hubei, China

³ School of Mathematics and Physics, China University of Geosciences (Wuhan), Wuhan 430074, Hubei, People's Republic of China

*Corresponding author: xbduan@wit.edu.cn, bshan@mail.hust.edu.cn

List of contents:

- Usage of constructed Pt-Rh potential
- Supplementary Figures and Tables

Usage of constructed Pt-Rh potential

The developed machine learning potential for the Pt-Rh system based on the DeePMD model can be obtained from the following link:

https://drive.google.com/file/d/1DV4Yu7ppldpY9F8xL_ZK2RELulDs-Y/view?usp=sharing

Usage Instructions:

To simulate a Pt-Rh system, follow these steps:

1. Download the potential file from the link above.
2. Place the potential file in the same directory as the LAMMPS script.
3. Include the following commands in the LAMMPS script to set up the potential:

```
pair_style deepmd Pt-Rh.pb  
pair_coeff * *
```

Important Notes:

1. Ensure that the order of elements in the atomic model is Pt, Rh.
2. The LAMMPS software must have the plugin that supports DeePMD installed. Specific installation instructions and further information can be found from the DeePMD community.

Table S1. Detailed information of the seven involved Pt-Rh nanoparticles.

Name	Property	Shape						
		CU	TO	IH	TD	DH	OH	SP
Pt₃Rh₁	Number of Pt atoms	1025	968	1064	961	1085	1095	967
	Number of Rh atoms	347	321	351	327	357	374	322
	Total number of atoms	1372	1289	1415	1288	1442	1469	1289
	Diameter (nm)	2.80	3.14	3.15	2.75	5.03	4.71	3.40
Pt₁Rh₁	Number of Pt atoms	689	641	710	646	720	732	645
	Number of Rh atoms	683	648	705	642	722	737	644
	Total number of atoms	1372	1289	1415	1288	1442	1469	1289
	Diameter (nm)	2.80	3.12	3.12	2.73	4.99	4.67	3.40
Pt₁Rh₃	Number of Pt atoms	337	321	360	324	361	359	309
	Number of Rh atoms	1035	968	1055	964	1081	1110	980
	Total number of atoms	1372	1289	1415	1288	1442	1469	1289
	Diameter (nm)	2.80	2.97	3.10	2.71	4.95	4.64	3.40

Table S2. Detailed statistical information used to construct the machine learning potential of the Pt-Rh system.

Structure type	Pt	Rh	Pt-Rh	Total
Bulk structures	1623	1623	1869	5115
Cluster structures	1062	1260	231	2553
Slab structures	600	600	1816	3016
Ordered structures	-	-	1000	1000
Total	3285	3483	4916	11684

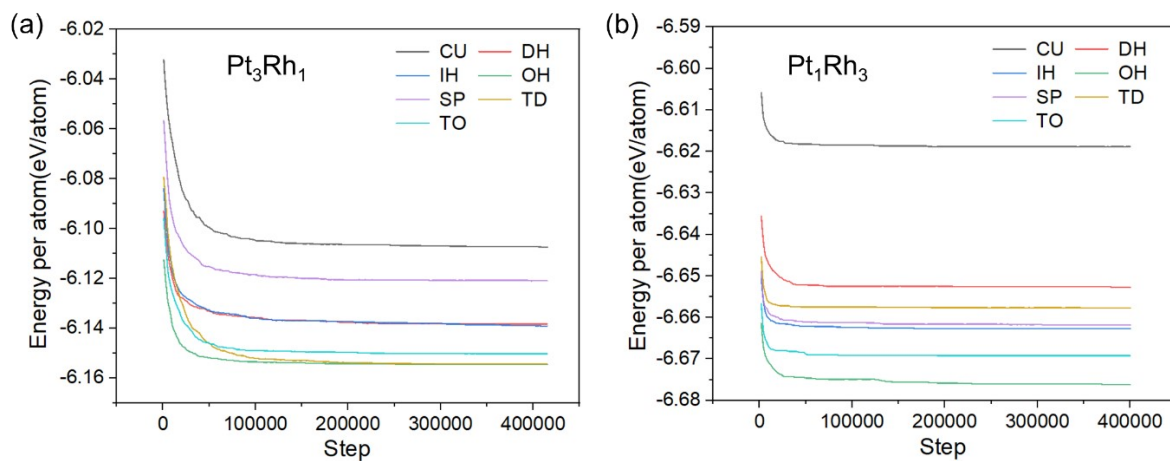


Fig. S1. Variation of the average atomic energy of (a) Pt_3Rh_1 and (b) Pt_1Rh_3 NPs with different shapes at 1K as a function of the simulation step.

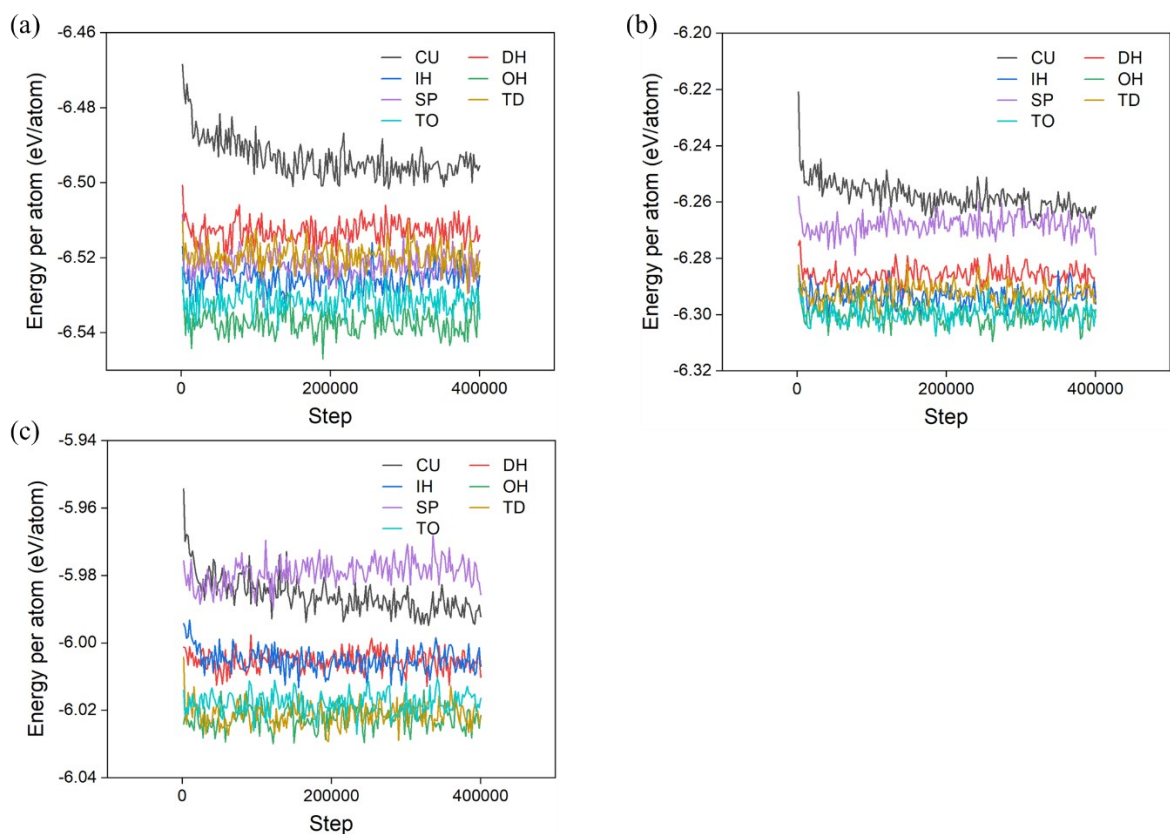


Fig. S2. Variation of the average atomic energy of (a) Pt_1Rh_3 , (b) Pt_1Rh_1 and (c) Pt_3Rh_1 NPs in 900K with different shapes at 900K as a function of the simulation step.

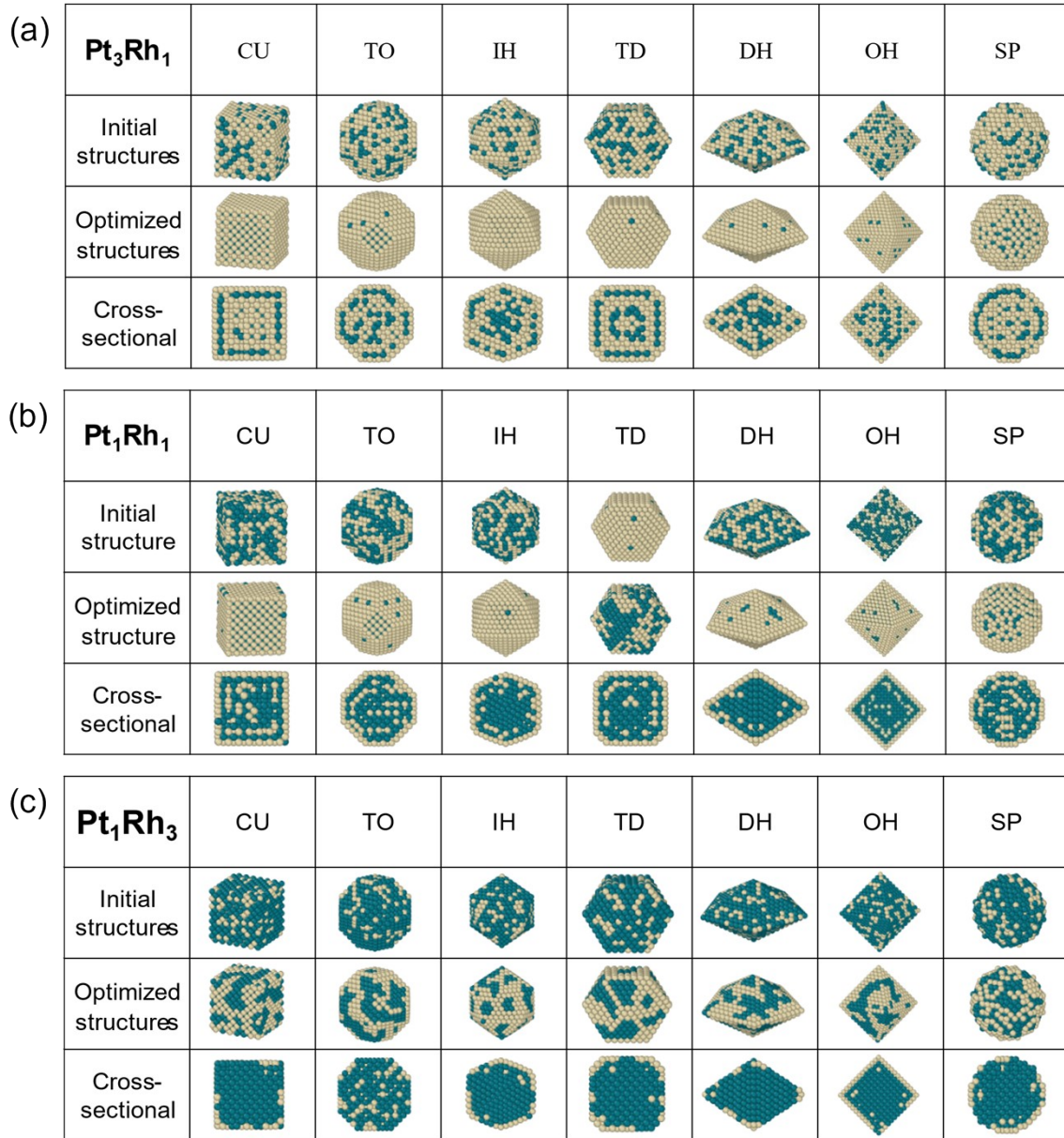


Fig. S3. Structural snapshots (including initial structures, optimized structures, and cross-sectional views) for (a) Pt_3Rh_1 , (b) Pt_1Rh_1 , and (c) Pt_1Rh_3 with different shapes.

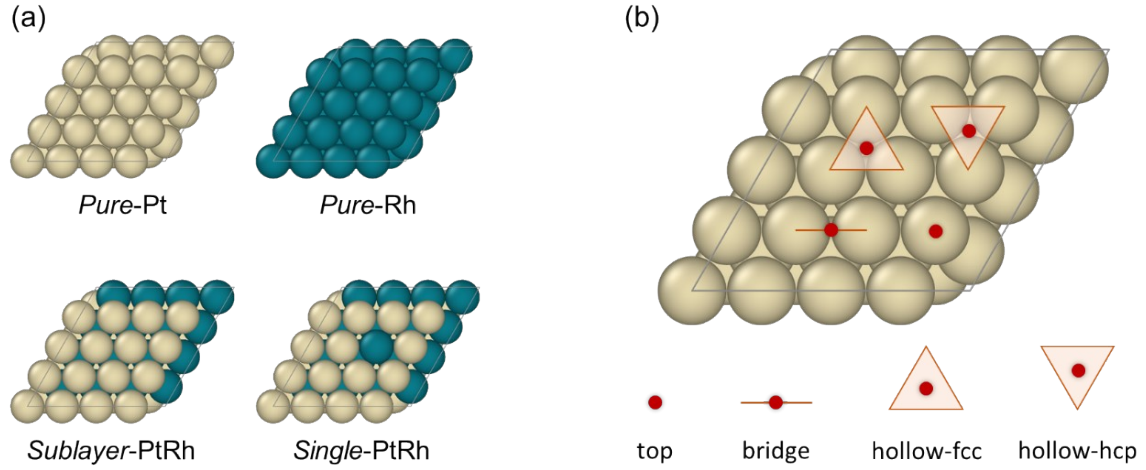


Fig. S4. (a) Four surface models constructed from the observed common morphology of the surface distribution of Pt-Rh NPs. (b) Schematic diagram of surface adsorption sites.

Table S3. Reaction pathways of N_2 recombination on four different surface models (including *Pure-Pt*, *Pure-Rh*, *Sublayer-PtRh*, and *Single-PtRh* surfaces), along with the corresponding reaction barriers (E_a) and reaction enthalpies (ΔE).

Surface model	Path	Reaction pathway	ΔE (eV)	E_a (eV)
<i>Pure-Pt</i>	I	N(fcc)+N(fcc) \rightarrow N ₂ (top)	-1.10	2.06
	II	N(hcp)+N(hcp) \rightarrow N ₂ (top)	-1.57	1.78
<i>Pure-Rh</i>	I	N(hcp)+N(hcp) \rightarrow N ₂ (top)	-0.04	2.23
	II	N(fcc)+N(fcc) \rightarrow N ₂ (top)	-0.28	2.00
<i>Sublayer-PtRh</i>	I	N(fcc)+N(fcc) \rightarrow N ₂ (top)	-1.44	1.96
	II	N(hcp)+N(hcp) \rightarrow N ₂ (top)	-1.74	1.76
<i>Single-PtRh</i>	I	N(fcc)+N(fcc) \rightarrow N ₂ (top)	-1.23	1.99
	II	N(hcp)+N(hcp) \rightarrow N ₂ (top)	-1.31	1.93

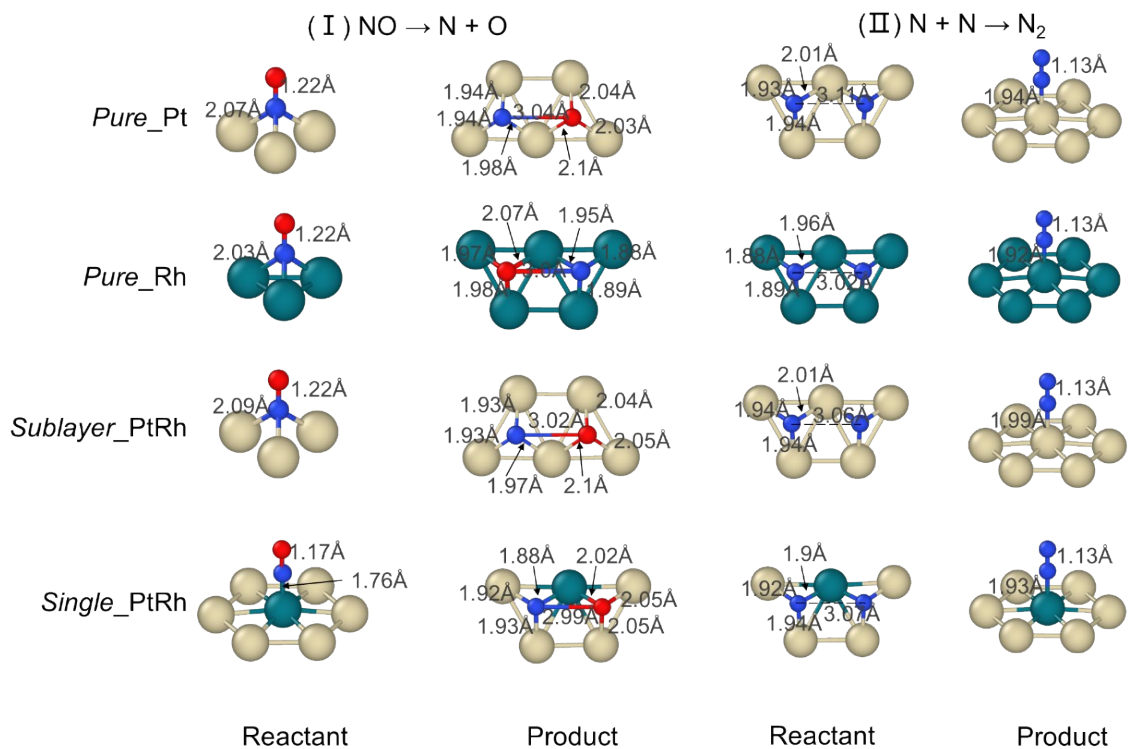


Fig. S5. Information on the geometrical structure of the initial and final states in the (a) NO dissociation and (b) N_2 recombination steps on four involved surface models.

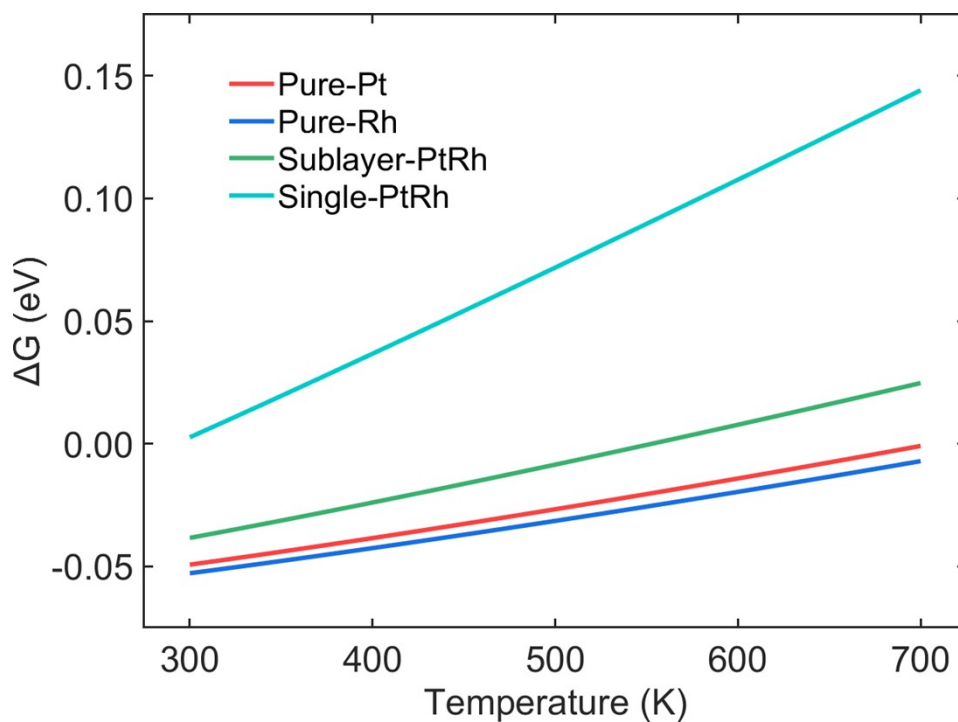


Fig. S6. Free energy corrections of NO dissociation barriers at 300K-700K.